

1 **A methodological framework for assessing and reducing temporal uncertainty in**
2 **paleovegetation mapping from late-Quaternary pollen records**

3

4 Jessica L. Blois^{1*}, John W. (Jack) Williams¹, Eric C. Grimm², Stephen T. Jackson³, Russell W.
5 Graham⁴

6

7 1. Department of Geography and the Center for Climatic Research, University of Wisconsin-
8 Madison, Madison, WI 53706 USA

9 2. Research and Collections Center, Illinois State Museum, Springfield, IL 62703 USA

10 3. Department of Botany and Program in Ecology, University of Wyoming, Laramie, WY 82071
11 USA

12 4. Earth and Mineral Sciences Museum, Pennsylvania State University, University Park, PA
13 16802 USA

14

15 *corresponding author; full contact information:

16 Center for Climatic Research

17 1225 W. Dayton St.

18 University of Wisconsin-Madison

19 Madison, WI 53706 USA

20 e-mail: blois@wisc.edu

21 telephone: 650-804-2934

22 fax: 608-263-4190

23 **Abstract**

24 Mapping past vegetation dynamics from heterogeneous databases of fossil-pollen records must
25 face the challenge of temporal uncertainty. The growing collection of densely sampled fossil-
26 pollen records with accurate and precise chronologies allows us to develop new methods to
27 assess and reduce this uncertainty. Here, we test our methods in the context of vegetation
28 changes in eastern North America during the abrupt climate changes of the last deglaciation. We
29 use the network of fossil-pollen records in the Neotoma Paleoecology Database
30 (www.neotomadb.org) and data contributed by individual investigators. Because many of these
31 records were collected decades before the current generation of ^{14}C and age-model technologies,
32 we first developed a framework to assess the overall reliability of ^{14}C chronologies by
33 systematically evaluating individual ^{14}C ages and associated chronologies. We developed a
34 qualitative ranking scheme for individual ^{14}C ages that combines information about their
35 accuracy and precision. ‘Benchmark’ pollen records were defined to have at least one ^{14}C age
36 with an accuracy within 250 years and a precision less than 500 years that is within 1,000 years
37 of the time interval of interest, and at least five pollen samples per 1,000 years across this time
38 period. Only 22 of >350 late-Pleistocene pollen cores in eastern North America met the
39 benchmark criteria. We then used Bayesian change-point analysis to identify widespread
40 ecological events (*Picea* decline, *Quercus* rise, and *Alnus* decline), and interpolated the ages of
41 these events from the benchmark sites to non-benchmark sites. Leave-one-out cross-validation
42 analyses with the benchmark sites indicated that the spatial error associated with interpolation
43 was less for inverse distance-weighting (IDW) than thin-plate splines (TPS) and was about 500
44 years for the three biotic events. By comparison, the difference between the original ages of
45 events at poorly constrained sites and the biostratigraphic ages interpolated from the benchmark

46 sites was close to 1000 years, suggesting that the use of biostratigraphic ages can significantly
47 improve the age models for poorly constrained sites. Overall, these analyses suggest that the
48 temporal resolution of multi-site syntheses of late-Pleistocene fossil-pollen data in eastern North
49 America is about 500 years, a resolution that allows analysis of ecological responses to
50 millennial-scale climate change during the last deglaciation.

51

52 Keywords: Neotoma; age model; Quaternary; paleoecology; pollen core

53 **1 Introduction**

54 Future climates are projected to warm substantially and rapidly (Solomon et al., 2007) and how
55 species and communities will respond to these changes is still uncertain. The paleoecological
56 record of past vegetation change is a powerful source of data for understanding potential
57 responses. The rates and magnitudes of abrupt climate changes such as the initiation of the
58 Bølling-Allerød event 14.5 thousand calendar years ago (ka) and the initiation and termination of
59 the Younger Dryas event (12.9-11.5 ka) (Denton et al., 2010) approximate those projected for the
60 21st century (Overpeck et al., 2003; Williams et al., in press); these time periods are thus critical
61 for studying ecological responses to abrupt climate change. Integrative analyses of
62 paleoecological records can help to answer questions about the velocity of species migration and
63 population expansion, changes in vegetation composition, ecological resilience to climate
64 change, and ecosystem responses to abrupt climate change (Dietl and Flessa, 2011; Flessa and
65 Jackson, 2005; Willis et al., 2010).

66

67 Mapped networks of fossil-pollen and plant-macrofossil data are the primary source of
68 information about spatial responses of plant species and communities to late-Quaternary climate
69 change. Thousands of pollen records from the late Quaternary have been collected globally and
70 are incorporated into public databases (APSA Members, 2007; Binney et al., 2008; Fyfe et al.,
71 2009; Grimm et al., 2007). Syntheses of these records have provided fundamental insights into
72 the relative sequence and nature of vegetation change over the past 21,000 years (e.g. Davis,
73 1976; Firbas, 1950; Huntley and Birks, 1983; Williams et al., 2004). Increasingly, these datasets
74 are used to determine the timing and rate of vegetation responses to rapid climate change (e.g.
75 Peros et al., 2008; Shuman et al., 2002). At local to regional scales, sites with paired vegetation

76 and climate records demonstrate that shifts in vegetation composition occurred within decades or
77 less of abrupt climate change (e.g. Birks and Ammann, 2000; Williams et al., 2002; Yu, 2007).
78 At sub-continental scales, late Quaternary vegetation has been mapped at 1000-year intervals
79 (Williams et al., 2004). These maps summarize the spatial patterns of vegetation dynamics when
80 forced by climate at orbital to millennial timescales, while rate-of-change analyses based on
81 these datasets show elevated rates of community turnover associated with the Younger Dryas
82 and Pleistocene/Holocene transition (Grimm and Jacobson, 1992; Jacobson et al., 1987; Shuman
83 et al., 2005; Williams et al., 2004).

84
85 These mapped syntheses, however, are critically limited by the accuracy and precision of the ^{14}C
86 ages and age models of the constituent pollen records (Grimm and Jacobson, 2003), which limits
87 their utility for studying climate-driven vegetation dynamics at sub-millennial scales. Most
88 pollen records used in these syntheses were developed before current methods of ^{14}C dating were
89 available and are based on sparse, inaccurate, and/or imprecise ^{14}C ages. Nevertheless, these
90 records contain unique information about local vegetation history and so there is value in
91 retaining them in integrative analyses.

92
93 An emerging challenge is to use the relatively precise chronological information available in a
94 small but growing set of fossil-pollen records with highly accurate and precise chronologies,
95 while also taking advantage of the spatial density of the full pollen databases. One way forward
96 is to use ecological events from the well-dated records as biostratigraphic markers to update the
97 age models of other, more poorly constrained pollen records. We first review sources of
98 temporal uncertainty in paleovegetation mapping, then outline a conceptual framework for

99 ranking the quality of individual ^{14}C ages and site chronologies that assesses both the random
100 and systematic sources of error (Section 2). In Section 3, we apply this framework to identify
101 the best pollen records (which we term ‘benchmark’ sites). We then use Bayesian change-point
102 analysis (Barry and Hartigan, 1993; Emerson and Erdman, 2007) to determine the timing of
103 widespread ecological events for the benchmark sites (the end-Pleistocene *Picea* decline,
104 *Quercus* rise, and *Alnus* decline). We reassess the timing of these ecological events at poorly
105 constrained sites by spatially interpolating the event ages from the benchmark sites to all sites
106 across the region. Although conceptually similar to using pollen-zone boundaries as a tool for
107 stratigraphic correlation (e.g., Deevey, 1939; von Post, 1946), the use of events linked to
108 individual taxa rather than to overall pollen assemblages is preferable because taxa respond
109 individualistically and their changes can be tracked over larger areas than pollen zones, which
110 are often definable only for limited spatial regions. Additionally, our method neither assumes
111 nor rejects synchrony of biological events (Blaauw, 2010b), but only assumes that these events
112 spatially propagate in a smooth manner. Maps of these events also provide an opportunity to
113 study the spatial velocity of major biotic changes. Finally, we quantify the temporal uncertainty
114 associated with individual sites and the spatial interpolation of ecological events and assess the
115 impact of the new biostratigraphic age estimates on the poorly constrained chronologies. These
116 analyses lay the foundation for a new generation of maps and other syntheses designed to
117 understand sub-millennial vegetation responses to rapid climate changes.

118

119 **2 Sources of Temporal Uncertainty in Paleovegetation Mapping**

120 Multiple sources of temporal uncertainty affect paleovegetation mapping. The quality of a
121 chronology for a site depends on the density of independent age controls, the accuracy and

122 precision of individual ^{14}C ages and other age controls, uncertainties in the ^{14}C calibration curve,
123 and uncertainties in age models. If biostratigraphic events are used as age controls, additional
124 uncertainty arises from the assumptions built into the spatial interpolation of ecological events
125 among sites. Simple assumptions that biostratigraphic events are synchronous are particularly
126 problematic (Blaauw, 2010b; Smith and Pilcher, 1973). Temporal uncertainties for individual
127 site chronologies accumulate when assembling data from many irregularly distributed sites
128 having chronologies of varying quality (Bennett, 1994; Bennett and Fuller, 2002). In order to
129 build and critically evaluate syntheses of past vegetation dynamics, all sources of temporal
130 uncertainty must be quantified and minimized.

131
132 We focus here on ^{14}C ages because these are by far the most common form of radiometric dating
133 for late-Quaternary pollen records. The quality of a ^{14}C age comprises two components:
134 precision and accuracy. Precision refers to the temporal width of the probability density function
135 (pdf) of a radiometric age. Here we define precision as the two-sigma or 95% highest posterior
136 density region of the calibrated ^{14}C age or other absolute age control. For ^{14}C ages, precision
137 depends on analytical precision and the shape of the calibration curve. The major constraint on
138 analytical precision is the amount of carbon in the sample and its age (Bronk Ramsey, 2008),
139 which is why small and old materials tend to have the worst precision. Analytical precision is
140 also affected by the dating method, particularly between conventional radiometric versus
141 accelerator mass spectrometry (AMS) ^{14}C dating. As technologies have improved, precision has
142 increased (Santos et al., 2007). For a ^{14}C age of a given analytical precision, the precision of the
143 calibrated age is highly dependent upon the shape of the calibration curve where intercepted by
144 the ^{14}C -age pdf. Because of variations in atmospheric ^{14}C through time (Damon et al., 1978), the

145 calibration curve is irregular and non-monotonic (e.g. Reimer et al., 2009). Wiggles in the curve
146 usually cause the pdfs of calibrated ages to be broader than their ^{14}C -age pdfs. However, if the
147 ^{14}C pdf intercepts a steep portion of the calibration curve, the calibrated ^{14}C age may be more
148 precise than the original measurement.

149
150 The accuracy of an age control is defined as the magnitude of any offset between the true age
151 and estimated age of an event. A ^{14}C age may be precisely measured, but inaccurate if the age of
152 the dated material does not correspond with the age of deposition. Accuracy depends upon the
153 type and amount of material chosen for ^{14}C dating, as well as stratigraphic integrity and
154 depositional processes. For a ^{14}C age to accurately estimate the true age, $\Delta^{14}\text{C}$ in the dated
155 sample must represent atmospheric $\Delta^{14}\text{C}$ at the time of deposition. Contamination in the field or
156 laboratory can bias the results, producing either too old or too young ^{14}C ages. Ages on small
157 amounts of material are more susceptible to contamination and thus inaccurate ages (Bronk
158 Ramsey, 2008). Perhaps an even more serious problem is that carbon in lake sediments can be
159 redeposited or derived from older sources. The well known “hardwater effect” results from
160 aquatic organisms such as algae and submersed aquatic plants incorporating ^{14}C -depleted carbon
161 derived from groundwater dissolution of carbonate rocks such as limestone and dolomite (e.g.
162 Andree et al., 1986; Deevey Jr et al., 1954; Grimm et al., 2009; MacDonald et al., 1991). The
163 hardwater effect is generally a problem with bulk-sediment ages, but also with shells from
164 ostracodes and mollusks, for example. On some landscapes, old carbon derived from extensive
165 peatlands (Lowe et al., 1988) may bias ^{14}C ages, and on some geological settings old carbon
166 from carbonaceous rocks such as shales and lignite may severely bias bulk-sediment ^{14}C ages—
167 by as much as 8000 years (Grimm et al., 2009).

168

169 Given these problems with bulk-sediment ages, terrestrial plant macrofossils are preferred now
170 for dating. However, terrestrial plant macrofossils may also provide inaccurate ages. Wood and
171 wood charcoal, although in principle excellent materials for ^{14}C dating, may exhibit “in-built”
172 ages because they may be derived from long-lived or long-dead trees (Gavin, 2001). Wood and
173 wood charcoal are resistant to decay and physical destruction and may persist for a long time
174 before transport to lake sediments (Barnekow et al., 1998; Gavin, 2001; Oswald et al., 2005). In
175 contrast, charcoal from short-lived herbaceous plants is much more delicate and may, in general,
176 provide more accurate ^{14}C ages (Grimm et al., 2009). But even terrestrial plant macrofossils well
177 suited for dating, such as small seeds and conifer needles, may be redeposited, perhaps from
178 shallower lake sediments (Grimm, 2011; Turney et al., 2000).

179

180 In most cases, accuracy cannot be determined directly because the true ages are not known.
181 However, accuracy can be qualitatively assessed based on expert knowledge of potential sources
182 of systematic bias. This assessment considers two sets of processes: those preceding the death or
183 excision of the material (i.e., residence time of the dated material in the living organism) and
184 those occurring from the time of death to deposition (i.e., residence time in the environment).
185 For example, residence times of seeds on a tree are on the order of one or at most a few years,
186 while stem wood may be derived from tissue formed from 10^0 to 10^3 years prior to tree death.
187 Once the tree’s tissues are released to the environment (e.g. through seedfall or tree death),
188 taphonomic processes determine the residence time before the material is transported and
189 permanently deposited in a sedimentary archive. Typical environmental residence times range
190 from 10^0 to 10^3 years, depending on the material and the depositional setting. For example,

191 transport and burial of an intact seed in lake sediments may have occurred within a year, whereas
192 wood fragments in a fluvial setting may have been deposited, reworked, and redeposited for
193 decades to centuries – or even millennia – before final deposition. Accuracy will be highest
194 when pre- and post-death residence times are minimal. With a sufficient number of ^{14}C ages
195 from a sedimentary sequence, large inaccuracies in any single age will usually be evident. More
196 difficult to detect are small errors of a few decades or centuries.

197
198 Major strides have been made in the past decade towards understanding the best material and
199 methods for dating pollen cores, for improving the precision of ^{14}C calibration curves (e.g. Bronk
200 Ramsey, 2008), and for constructing age models (e.g. Blaauw, 2010a; Parnell et al., 2008). A
201 new generation of fossil-pollen records with high-precision ^{14}C ages on carefully chosen organic
202 carbon has been collected over the last decade [e.g., Kettle Lake (Brown et al., 2005; Clark et al.,
203 2002; Grimm, 2011), White Lake (Yu, 2007)]. However, many records contain very few (or no)
204 radiometric ages, and many of the existing radiometric ages may be inaccurate. One option is to
205 simply discard these records, but this practice eliminates considerable information because each
206 site is a unique record of vegetation history at a particular locale. Alternatively, the age models
207 for these records can be reassessed and refined by using non-radiometric age controls such as
208 biostratigraphic events. In this approach, the ages of major ecological events at well-dated sites
209 are spatially interpolated to other sites and used as age controls for the chronologies of these
210 sites. This procedure introduces new complications, particularly that age models based on
211 biostratigraphic ages are no longer fully independent of age models from other sites and thus
212 incorporate assumptions about spatiotemporal propagation of ecological events (Blaauw, 2010b).
213 Furthermore, many methods are available for spatially interpolating events between sites, and

214 interpolation precision may vary based on technique, so a new source of uncertainty emerges
215 when transferring ages of ecological events at individual sites to nearby sites: error due to the
216 method of spatial interpolation.

217

218 *2.1 Conceptual framework for determining benchmark chronologies*

219 The framework developed here explicitly accounts for and limits many of the above sources of
220 error. There are three main elements: 1) a system for ranking the quality of individual ages,
221 based on their accuracy and precision, 2) a system for identifying benchmark chronologies, and
222 3) methods for identifying major ecological events, interpolating the ages of events to other sites,
223 and quantifying the error of spatial interpolation for the resultant biostratigraphic ages. We
224 outline the criteria used to rank ^{14}C ages and identify benchmark sites here, then develop the
225 interpolation methods in *Section 3*.

226

227 Our framework for ranking the quality of individual ages (Table 1) jointly addresses the issues of
228 accuracy and precision outlined above. Because accuracy is rarely known, we developed a
229 qualitative ranking scheme (Table 1) and assigned ranks to individual ^{14}C ages based on their
230 material and depositional setting (Appendix A). We also converted precision into a qualitative
231 ranking, scaled to be comparable to the accuracy rankings. Our ranking categories capture a
232 wide range of possible accuracies and precisions and can be extended further as needed.

233

234 After each ^{14}C age was coded for accuracy and precision, we developed a set of criteria to
235 identify benchmark sites, i.e. sites with the most accurate and precise temporal resolution. The
236 density and quality of ages and sampling resolution varies within sites, so some sites may be

237 benchmarks for one time period, but not another. Because our objective is to map sub-
238 millennial-scale ecological phenomena, we defined a benchmark site according to the following
239 criteria: a) the chronology contained, within 1000 years of the time period of interest, at least
240 one AMS ^{14}C age with an accuracy rank ≤ 4 (i.e., on terrestrial material with a short residence
241 time, such as seeds, twigs, and cones) and precision rank ≤ 5 (a calibrated 95% confidence
242 interval <500 years) (Table 1); b) the time period contained at least 5 pollen samples per 1000
243 years. The only non-radiometric ages allowed in benchmark chronologies were core tops and the
244 ages of the European settlement (e.g. marked by a rise in *Ambrosia* pollen), though these markers
245 were largely irrelevant here since this paper focuses on the late Pleistocene. This definition of a
246 benchmark was designed for our specific research objectives and may be too restrictive (or too
247 loose) for other applications.

248

249 **3 Materials and Methods**

250 *3.1 The Neotoma Paleoecology Database*

251 We focus on lake-sediment records from eastern North America in the Neotoma paleoecology
252 database (www.neotomadb.org). Neotoma is a multiproxy relational database that stores fossil
253 data for the past 5 million years (the Pliocene and Quaternary). The fossil-pollen component of
254 Neotoma currently comprises over 4,200 sites globally, with almost 400 additional sites
255 submitted and awaiting data upload. We limited our search to records with pollen data between
256 21 and 11.5 ka; we will soon extend our effort to the Holocene. Overall, 371 sediment cores
257 were included in this analysis (Figure 1).

258

259 *3.2 Ranking the quality of individual ages and defining benchmark sites*

260 We assessed the quality of all ^{14}C ages and defined benchmark sites according to the criteria
261 outlined in 2.1. Each ^{14}C age was assigned an accuracy ranking based on the type of the dated
262 material (Table 1, Appendix A). The precision of each ^{14}C age was calculated based on the 95%
263 confidence interval of the calibrated age and converted into a qualitative ranking (Table 1). All
264 ages were calibrated in Calib 6.0 (Stuiver and Reimer, 1993) using the IntCal09 calibration curve
265 (Reimer et al., 2009). For non-radiometric ages, such as core tops or cultural associations, the
266 precision rank was calculated from the author-determined age range.

267

268 *3.3 Age models*

269 Except where noted (section 3.7), we relied on the default Neotoma chronologies, particularly
270 regarding the shape of the age model (e.g., linear interpolation vs. polynomial) and decisions
271 about which ^{14}C ages were rejected or averaged. Neotoma's defaults were developed by either
272 the original researchers, previous working groups, or by the Neotoma data steward upon data
273 upload. These chronologies are based largely on radiometric ages (mostly ^{14}C) from diverse
274 source materials and biostratigraphic markers. Neotoma stores age estimates but not age-model
275 uncertainty for each sample within a pollen record. We estimated the chronology error for
276 samples by assigning the maximum 2-sigma calibrated age range of the age controls bracketing
277 each pollen sample to the estimated sample ages and assumed a uniform error distribution within
278 this age range.

279

280 We explicitly chose not to override the expert knowledge that went into creating the original age
281 model at a site, unless we had information not available to the original authors (e.g. the IntCal09
282 calibration curve). However, we tested the effect of simply updating the default age model to

283 IntCal09 versus constructing a Bayesian age model by comparing the Neotoma chronologies
284 with chronologies constructed in Bchron (Supplementary Discussion, Supplementary Figures
285 1,2; Haslett and Parnell, 2008; Parnell et al., 2008). The expected values of the original and
286 Bayesian models generally show only small differences (<200 years), mainly because Bayesian
287 approaches have little impact unless the pdfs of the calibrated radiocarbon ages overlap enough
288 to constrain each other (Supplementary Figure 1). There were also no systematic differences in
289 uncertainty surrounding the event ages between the two types of chronologies, although a few
290 sites showed larger uncertainties in the Bayesian estimates of age ranges at some ecological
291 events (Supplementary Figure 1).

292

293 *3.4 Determining significant biostratigraphic events*

294 We used a combination of Bayesian change-point analysis and visual analysis to identify
295 biostratigraphic events at all cores. Five end-Pleistocene biostratigraphic events were selected *a*
296 *priori*, based on their widespread occurrence in eastern North America: *Picea* decline, *Alnus* rise
297 and decline, *Pinus* rise, and *Quercus* rise (Mayle et al., 1993a; Williams et al., 2004). For
298 example, we scanned each time series of *Picea* pollen abundance at benchmark sites to
299 determine if there was a change point associated with the final decline in *Picea* near the end of
300 the Pleistocene (Figure 2). Not all sites manifest each event. We used the R package BCP
301 (Emerson and Erdman, 2007) to determine change points. BCP implements a Bayesian analysis
302 (Barry and Hartigan, 1993) that partitions the time series of relative abundance data into
303 segments such that the mean relative abundance is constant within segments. We used 1000
304 Markov Chain Monte Carlo (MCMC) iterations with a burn-in period of 100 iterations, and set
305 the prior variance equal to the observed variance for the entire core. For each sample in the time

306 series, BCP determines the posterior probability that the sample is a change point, i.e. a point of
307 significant change in abundance between two segments of different mean abundances. The
308 change-point analyses typically find a few intervals with a high probability of being a change
309 point and most with a low probability (Figure 2).

310

311 For benchmark sites, we set an initial threshold of ≥ 0.80 posterior probability to identify change
312 points and visually inspected the relative abundance plot to determine which change point, if
313 any, was associated with a particular biostratigraphic event. We relaxed the 0.80 threshold for a
314 few cases in which we were both visually confident of an event and the BCP analysis detected a
315 lower probability change point, which happened for several time series for each ecological event
316 (>0.6 probability threshold for the *Alnus* decline at Splan Pond, and the *Quercus* rise at Clear
317 Pond, Hiscock Site, Sutherland Pond, and White Lake, and >0.3 probability threshold at Chase
318 Pond for the *Alnus* decline; Supplementary Information). Our identification of change points is
319 thus primarily determined by statistical methods but unavoidably includes some degree of
320 judgment. So that others can review our decisions, Supplementary Figure 3 shows the relative
321 abundance diagrams for the relevant pollen types for all benchmark sites, with our decisions
322 about which change points were associated with an event at each site. For non-benchmark sites,
323 we used the same change-point analysis procedure to determine the depths of the biostratigraphic
324 events, but adhered to a strict 0.80 posterior probability threshold.

325

326 *3.5 Spatially interpolating the ages of biostratigraphic events to other sites*

327 We inferred the mean age of an ecological event at each poorly constrained site by interpolation
328 among benchmark sites. We compared the performance of two spatial interpolation techniques:

329 inverse distance weighting (IDW) and thin-plate spline (TPS) interpolation. For IDW, inverse
330 distance power was set to 2. For TPS, we set the appropriate smoothing parameter (λ) by
331 generalized cross validation. For both IDW and TPS, we experimented with two sets of spatial
332 parameters for the interpolation: latitude and longitude (which we call 2d), and latitude,
333 longitude, and altitude (3d). All latitude and longitude coordinates were converted to North
334 America Albers Equal Area Conic projection (Origin: 40°N, 96°W, standard parallels: 20°N,
335 60°N). Altitude was upweighted in the 3d interpolation by using a scaling factor set to the
336 approximate ratio of the temperature lapse rate across latitude versus elevation in eastern North
337 America (1-km elevation \approx 600-km latitudinal distance) (Hopkins, 1920; MacArthur, 1972).
338 Because the sample depth of each ecological event in the benchmark sites was associated with an
339 age plus estimated uncertainty (see 3.3), we randomly drew an age of the change point from the
340 uniform age range associated with the event depth and repeated the IDW and TPS analyses 1000
341 times to calculate mean interpolated ages.

342

343 *3.6 Cross-validation*

344 To estimate error in the benchmark sites associated with spatial interpolation, we used a leave-
345 one-out cross-validation analysis in which we sequentially dropped each benchmark site from the
346 dataset and used the remaining benchmark sites to estimate the mean event age at the dropped
347 site. We used the same bootstrapping procedure with 1000 replicates as in section 3.5. We then
348 calculated the site cross-validation error by determining the difference between the original age
349 of the event estimated by change point analysis and the mean interpolated age of the event at the
350 dropped site. We used mean absolute error (MAE) to summarize cross-validation error across all
351 sites. Additionally, sites were classified as interpolation or extrapolation sites based on whether

352 they were located within or on the boundary of a minimum convex polygon around all sites.
353 (During cross-validation, removing a site that lies on this boundary forces the interpolation
354 technique to extrapolate to it from the other remaining sites.) We recalculated MAE for the
355 boundary and internal sites separately, which provided measures of extrapolation and
356 interpolation error. Interpolation error is the most relevant diagnostic, because biostratigraphic
357 ages were only assigned to non-benchmark sites if they lay within the minimum convex polygon
358 (i.e., we did not allow extrapolation). We also examined the error statistics for systematic bias
359 by correlating the site cross-validation error with five site characteristics: the original age of the
360 event, temporal sampling resolution at the time of the event, latitude, longitude, and altitude. For
361 each event, we also determined the influence of potential outliers on interpolation reliability.

362

363 *3.7 Impact of the new biostratigraphic age estimates on chronologies*

364 To assess the influence of the new biostratigraphic age estimates on chronologies, for each site
365 we compared the mean age of an event based on interpolation between the benchmark sites to the
366 age estimate based on the original chronology. In order to strictly limit this comparison to the
367 effects of the interpolation, we slightly modified the original chronologies by recalibrating all
368 age controls within the Neotoma default age model to the IntCal09 calibration curve and
369 recalculated ages at individual sampling depths. For this comparative analysis, we only used
370 cores with at least two ^{14}C ages and we removed all non- ^{14}C -based ages (such as deglaciation
371 ages, or age of the *Tsuga* decline) from the analysis except for core-top and *Ambrosia*
372 rise/European settlement. The form of the age model (e.g., linear interpolation, polynomial) was
373 unchanged from the original age model. Once the age model was updated, we extracted the ages
374 associated with the change point depths.

375

376 All analyses (change point detection, interpolation and cross-validation) were done using the
377 statistical package R (R Development Core Team, 2010). Copies of the scripts used for change
378 point determination and event age interpolation and cross-validation are provided in the
379 Supplementary Information.

380 **4 Results**

381 *4.1 Determining benchmark sites*

382 We searched Neotoma for all North American pollen records east of the Rocky Mountains with
383 ^{14}C ages, focusing on lake and mire depositional environments (Figures 1, 3). This search
384 provided a list of initial sites ($n=371$) with over 3150 associated ^{14}C ages (Appendix B). Of
385 these sites, 297 sites had sufficient chronological information for this project (e.g. at least 2 valid
386 age controls to interpolate ages to undated samples), but only 17 sites met all criteria for being a
387 benchmark site for at least part of the late Pleistocene (Figure 1). To this list, we added three
388 sites because their chronologies nearly met the benchmark site criteria, and they filled important
389 regional or temporal gaps: Brown's Pond, Cottonwood Lake, and Sharkey Lake. The
390 chronology for Brown's Pond, VA (Kneller and Peteet, 1993) did not meet the age precision
391 criterion; it had one good age (accuracy rank=2, precision rank=5) at 8.5 ka, among other lower-
392 quality ages. However, this site clearly fills an important spatial gap (Figure 3). Cottonwood
393 Lake, SD (Barnosky et al., 1987; Grimm et al., 2009) also fails the precision threshold, with one
394 good age at 8.6 ka, but this site increases site density in the sparsely sampled western region of
395 the dataset (Figure 3). Sharkey Lake, MN (Camill et al., 2003) did not meet the sampling
396 density criterion (roughly 4 samples per 1000 years rather than 5), but this site bridges a gap
397 between sites close to Great Lakes and sites farther west so we retained this site as well (Figure
398 3). Additionally, two sites met most criteria, but their sampling did not extend into the late
399 Pleistocene (21-11.5 ka) [Blackwoods Hollow, ME (Schauffler and Jacobson Jr, 2002) and Steel
400 Lake, MN (Tian et al., 2005; Wright et al., 2004)]. These sites were used in cases when
401 ecological events extended into the early Holocene. Overall, we identified 22 benchmark sites

402 (Figures 1, 3). Even given the expanded final list of benchmark sites, the spatial and temporal
403 density of these sites varied greatly (Figure 3).

404
405 The highest density of benchmark sites was found in the time period 12.9-11.5 ka (22 sites), and
406 benchmark sites for other late-Pleistocene time periods were subsets of this list (Figure 3). The
407 number of benchmark sites declined with increasing age (14.5-12.9 ka: 18 sites; 18-14.5 ka: 8
408 sites; 21-18 ka: 4 sites). The percentage of benchmark sites ranged from 8.5% to 14% among the
409 four time periods (12.9-11.5 ka: 22/223 sites; 14.5-12.9 ka: 18/153 sites; 18-14.5 ka: 8/94 sites;
410 21-18 ka: 4/28 sites). Given the paucity of sites in the earlier time periods, we focused
411 exclusively on the latest Pleistocene (12.9-11.5 ka) in examining biostratigraphic events.

412

413 *4.2 Biostratigraphic events and cross-validation*

414 Of the five ecological events initially examined (*Alnus* rise, *Alnus* decline, the end of *Picea*
415 decline, *Pinus* rise, and *Quercus* rise), we eliminated the *Pinus* rise because not all researchers
416 discriminated between *P. strobus* (subg. *Strobus*) and *P. banksiana/resinosa* (subg. *Pinus*), and
417 the *Alnus* rise because spatial cross-validation error indicated it was a poorly constrained event.
418 Thus, our final analysis included *Alnus* decline, *Picea* decline, and *Quercus* rise. For all three
419 events and across all interpolation methods, error was significantly correlated with the original
420 age of the event at sites, indicating that the interpolated ages are smoothed and hence have less
421 variance than the original ages (Table 2). Error was not consistently correlated with temporal
422 sampling resolution, nor with spatial attributes such as latitude, longitude, or altitude (Table 2).
423 Additionally, for both the IDW and TPS interpolation techniques, using altitude did not
424 significantly increase interpolation accuracy and in some cases worsened it, so for simplicity we

425 present results for interpolation using latitude and longitude only (e.g. IDW-2d and TPS-2d).
426 We applied the interpolated ages to all poorly constrained sites within a minimum convex
427 polygon that spanned the benchmark sites used for interpolation.
428
429 Across all events, IDW-2d interpolation had a smaller cross-validation error than TPS-2d
430 interpolation (e.g., 574 years Interpolation MAE vs 746 years Interpolation MAE for *Picea*
431 decline; Table 3). TPS-2d smoothed the pollen signal more strongly and was more highly
432 influenced by individual sites (Figure 4). The means of the interpolated ages did not
433 substantially differ between IDW-2d and TPS-2d, though in general IDW-2d error was less than
434 TPS-2d error: *Picea* decline, -150 ± 256 (mean and standard deviation of the difference between
435 IDW-2d and TPS-2d ages, for both the benchmark and poorly constrained sites); *Alnus* decline,
436 18 ± 170 ; *Quercus* rise, -102 ± 392 . When using the IDW-2d interpolation method, cross-
437 validation interpolation error was less than 600 years for each event and lower than 400 years for
438 *Alnus* decline (Table 3, Interpolation MAE). The error estimates are highly influenced by a few
439 ‘outlier’ sites [i.e. Clear Pond (Hussey, 1993) for all three events, plus Brown’s Pond (Kneller
440 and Peteet, 1993) for *Alnus* decline; Table 3]. When outlier sites are removed, spatial
441 interpolation error (for the IDW-2d method) declines to 530 years for the *Picea* decline and 327
442 years for the *Alnus* decline, and increases to 614 years for the *Quercus* rise (Table 3). These
443 outlier sites generally occur in the south-central US in areas of low sampling density. The high
444 cross-validation errors for these sites are likely caused by a combination of time-transgressive
445 ecological events that are difficult to reproduce accurately when sites from low-density regions
446 are removed during the cross-validation, and possibly also errors in the age models for these sites
447 (Jackson and Whitehead, 1993; Jackson et al., 2000). Thus, these outlier sites cannot be well

448 predicted during the cross-validation analyses but, because they are in areas of low site density,
449 are essential to estimating biostratigraphic ages for the non-benchmark sites. We report error
450 estimates with and without these outlier sites (Table 3) and retain them in subsequent analyses.

451

452 *4.3 Comparison with original event ages*

453 The timing of biostratigraphic events estimated from the original chronologies of non-benchmark
454 sites varied widely (Table 4, Figure 5), and was often very different than age estimates based on
455 interpolation. For all events, the mean absolute age difference between interpolated ages (IDW-
456 2d) and original ages of the non-benchmark sites was approximately twice as much as the
457 Interpolation MAE of the cross-validation for the benchmark sites (Tables 3, 4): 845 vs. 574
458 years for *Picea* decline, 858 vs. 352 years for *Alnus* decline, 1106 vs. 573 years for *Quercus* rise.
459 This discrepancy indicates that error is built into many of the original site chronologies and the
460 interpolation of biostratigraphic ages can substantially improve these chronologies.

461

462 *4.4 Ecological patterns*

463 Although the primary focus of this paper is methodological, maps of the spatial propagation of
464 major biotic events reveal highly individualistic ecological dynamics (Figures 4, 6). For
465 example, the *Picea* decline and the *Quercus* rise both originated at southern sites between 16-18
466 ka and propagated northward. However, the *Picea* decline spread rapidly across the southern
467 Great Lakes region between 11.5 and 11 ka and then propagated west and northeast until the
468 final declines around 10.1 ka. On the other hand, the rise in *Quercus* abundances spread rapidly
469 through the northeast starting around 12 ka, but did not begin around the Great Lakes and
470 westward until after 11 ka. It did not rise at some sites until 9.1 ka. Thus, the temporal

471 relationship between *Picea* decline and *Quercus* rise varies spatially, in which the temporal
472 offset increases towards the northwest (Figure 6). In contrast to both events, the *Alnus* decline
473 originated much later (11.6 ka) than the other two events and occurred first in the northeast, then
474 spread south and west within a few hundred years. In New England and Maritime Canada, the
475 *Alnus* decline is an indicator of the end of the Younger Dryas (Mayle et al., 1993a), but these
476 maps suggest that across eastern North America, the *Alnus* decline is a rapid but time-
477 transgressive event.
478

478 **5 Discussion**

479 Spatial networks of well-dated fossil-pollen records are critically needed to understand spatial
480 vegetation dynamics during periods of abrupt change. We have 1) developed a methodological
481 framework that presents a standard ranking scheme for assessing the quality of ^{14}C ages and
482 outlines criteria for identifying benchmark sites, 2) applied this framework to identify benchmark
483 fossil-pollen records in eastern North America, and 3) used these benchmark sites to interpolate
484 the ages of key biostratigraphic events to other, less-well dated sites. We explicitly tested the
485 strengths and limits of this approach, focusing on late-Pleistocene pollen datasets from eastern
486 North America. Our cross-validation analyses show a mean error of roughly 500 years
487 associated with the spatial interpolation of key biostratigraphic events, suggesting that 500 years
488 is effectively the temporal limit to maps and other inter-site syntheses relying on late-Pleistocene
489 pollen records from eastern North America. To reduce error further and better understand the
490 spatial responses of plant taxa and communities to the abrupt climate changes accompanying the
491 last deglaciation, additional pollen records with high-resolution chronologies are critically
492 needed. In the meantime, this approach provides a simple yet rigorous way of assessing
493 temporal uncertainty and studying vegetation changes at sub-millennial timescales.

494

495 *5.1 Benchmark chronologies*

496 Many formal and informal approaches have been developed to evaluate reliability of individual
497 ^{14}C ages (Meltzer and Mead, 1983; Pettitt et al., 2003; Stafford Jr et al., 1987) and chronologies
498 (Jackson et al., 2000; Williams et al., 2004). We integrated information from various sources
499 into a comprehensive ranking scheme that is applied here to ^{14}C dating, but in principle is widely
500 applicable to different proxy types and dating methods.

501
502 The main elements of our framework are a) a qualitative scale that assesses both precision and
503 accuracy, b) a definition of benchmark sites that is tied to this scale, and c) standards for sample
504 density and age proximity. Other research groups have developed frameworks that contain
505 similar elements. For example, the European Pollen Database (EPD) has implemented a system
506 whereby each individual sample in a stratigraphic sequence is classified according to its temporal
507 uncertainty (Thomas Giesecke, pers. comm.). The EPD system takes into account the proximity
508 of ages to samples, as well as the overall shape of the age model in the region surrounding the
509 sample. The uncertainty of samples is estimated by linear interpolation of error at the bounding
510 ages, but accuracy and precision of the underlying ^{14}C ages are not formally assessed. The main
511 distinction between approaches is that the EPD is mainly concerned with characterizing the
512 temporal uncertainty of samples within a sequence, whereas we have focused on both assessing
513 the uncertainty of individual age controls and chronologies and narrowing that uncertainty by
514 incorporating biostratigraphic age estimates for poorly constrained chronologies. Our approach
515 is closer to that outlined in Williams et al. (2004), where individual sites were excluded or down-
516 weighted for mapping purposes by the age controls and sampling quality associated with the site.
517

518 After evaluating all late Pleistocene pollen datasets from eastern North America in the Neotoma
519 database, we found that only 22 of the several hundred datasets fulfilled the criteria for
520 benchmark sites (Figures 1, 3). This estimate is undoubtedly conservative. For example, we
521 have assigned an accuracy ranking of 5 (<500 years) to all ages obtained from bulk-sediment
522 samples, due to concerns about potential hardwater contamination, but in regions without known
523 hardwater effects, some sites that use AMS dating on bulk lake sediments may have accurate

524 chronologies (e.g., Blood Lake; Oswald et al., 2007). Our ranking assignments for individual
525 dates will be stored in Neotoma, so future workers can review and revise as appropriate. The
526 distribution of late Pleistocene benchmark sites in eastern North America is heavily concentrated
527 in the upper Midwest and Northeast, in part because of the large number of lakes in these
528 regions. However, suitable sites with good late Pleistocene records do exist in other regions that
529 should be a priority for re-dating [e.g. the southeastern United States (Jackson and Whitehead,
530 1993; Watts, 1980)]. The geographic bias of benchmark sites limits our ability to accurately
531 infer the rates and patterns of vegetation change across eastern North America and points to the
532 need for new sediment cores or new ages from existing cores in the undersampled regions.

533

534 *5.2 Quantifying and minimizing temporal error*

535 After accounting for both chronologic and interpolation error, the error associated with mapping
536 each ecological event was on the order of 500 years. This value indicates that the temporal
537 resolution of mapping can be improved to 500-year intervals for some periods of the late
538 Pleistocene, which is sufficient to detect ecological change before and after major events such as
539 the Bølling-Allerød and Younger Dryas oscillations. However, it also points to a temporal limit
540 to current synoptic mapping efforts, set by the site-specific variability of ecological events and
541 by error due to factors such as ^{14}C dating, calibration, and sampling resolution (both within core
542 and across landscape). The accumulated error during syntheses is too large to detect phenomena
543 that can be seen in individual well-dated records, e.g. the 300 to 400 year lag between local
544 climate changes at Crystal Lake, Illinois (Gonzales and Grimm, 2009) and the timing of Bølling-
545 Allerød and Younger Dryas oscillations in North Atlantic records. (However, leads and lags
546 could be calculated from individual well-dated records, then their spatial distribution mapped,

547 which would aid understanding of the teleconnections between North Atlantic and North
548 American climate).

549
550 The assignment of ages to biostratigraphic events at poorly constrained sites using IDW
551 interpolation clearly improved over the original age estimates for most of the original
552 chronologies (Table 4, Figure 5). For example, the mean absolute difference between the age of
553 the *Picea* decline based on interpolation versus its age from the original chronology is 845 years,
554 with individual differences ranging from interpolated ages 4353 years older than the original
555 chronology to 2889 years younger than the original chronology (Table 4). Some of this error is
556 due to interpolation, but the fact that the mean absolute age difference is substantially larger than
557 the mean cross-validation error for all events (Tables 3, 4) indicates that the use of
558 biostratigraphic ages roughly halves the temporal uncertainty inherent in the original
559 chronologies of some of the non-benchmark sites.

560
561 Critically, our method does not assume synchrony of biological events (Blaauw, 2010b; Smith
562 and Pilcher, 1973), but rather assumes that these events spatially propagate in a smooth manner.
563 A key innovation used here is change-point analysis, which offers a formal tool for determining
564 if and where particular biotic events occur in pollen records. This method avoids setting
565 arbitrary relative-abundance thresholds for particular events and instead focuses on the pattern of
566 change in each taxon within the context of the local site. Moreover, using change-point
567 detection for individual taxa, rather than pollen zonation based on the entire assemblage, is a
568 better way of accommodating individualistic species dynamics in data syntheses at sub-
569 continental and broader scales. Our use of biostratigraphic ages does build in assumptions about

570 the spatial smoothness of ecological change. Thus, the full dataset is appropriate for some
571 synthetic applications— e.g. data-model comparisons to vegetation models driven by global
572 climate models— but we must restrict ourselves to the benchmark sites and their independent
573 age models when testing hypotheses about spatiotemporal patterns within the taxa used as
574 biostratigraphic markers.

575
576 Our treatment of the sample-level temporal uncertainty resulting from age models was simple—
577 we assigned the maximum age range from the bracketing ages to a sample and assumed a
578 uniform age distribution around this sample (see *section 3.3*). New Bayesian age-modeling tools
579 (Parnell et al., 2008) allow integration of the age-calibration step with age-model construction
580 and provide posterior estimates of the age error of undated samples. The functionality to store
581 these estimates of sample-level age uncertainty is currently being built into the Neotoma
582 database. Because our estimates of sample-level uncertainty are intentionally conservative (i.e.
583 they likely overestimate uncertainty), incorporation of these new tools should reduce the
584 estimates of temporal uncertainty.

585

586 *5.3 Spatial patterns in major biotic events during the last deglaciation*

587 The events mapped here are broadly concordant with patterns identified previously (Williams et
588 al., 2004), yet refine key details of vegetation changes around abrupt climate events such as the
589 end of the Younger Dryas Chronozone. (It is difficult to compare strictly these maps with those
590 in Williams et al. (2004) because we are mapping different phenomena [pollen isochrones in this
591 paper versus isopolls in Williams et al. (2004)].) Both sets of maps show that the final decline of
592 *Picea* was time-transgressive, occurring first in the southern US, then very rapidly propagating

593 across in the northeastern US and eastern Great Plains (Figures 4, 6). Ages for this event among
594 the benchmark sites ranged from 16 ka at Clear Pond (Hussey, 1993) in the south to 10.15 ka at
595 Sharkey Lake (Camill et al., 2003) in the Upper Midwest.

596

597 Similarly, our mapping of the *Quercus* rise based on change-point detection (Figures 4, 6) is
598 broadly consistent with the Williams et al. (2004) maps but provides additional detail, showing
599 that the *Quercus* rise began in the northern US in western New York ca. 12 ka at the Hiscock
600 Site (McAndrews, 2003), then propagated through New England and Maritime Canada between
601 11.75 and 10.7 ka and westward through the Great Lakes between 11.9 ka and 9.1 ka. The value
602 of the improved sub-millennial temporal resolution is most notable for the *Alnus* decline. The
603 rise and decline of *Alnus* along the northeastern US and maritime Canada is effectively a
604 synchronous event that has been used as a biological indicator for the Younger Dryas
605 Chronozone (Mayle et al., 1993a). Our results confirm the synchrony of the *Alnus* decline along
606 the east coast around 11.5 ka, but also show that the *Alnus* decline then propagated westward
607 very quickly within a 1000 year interval (Figures 4, 6), reaching Sharkey Lake (Camill et al.,
608 2003) by 10.6 ka. This pattern suggests additional complexity to an ecological event that
609 previously had been linked simply to a single abrupt climate event. However, additional
610 taxonomic resolution may potentially reveal an even more complex event. In the maritime
611 provinces of Canada and highland areas of New England, the *Alnus* peak is primarily *A. viridis*-
612 type, whereas it is mainly *A. incana*-type at lowland sites (Mayle et al., 1993a). In the Midwest,
613 the *Alnus* peak is virtually all *A. incana*-type (e.g. Cushing, 1967; Gonzales and Grimm, 2009).
614 In addition, in the Northeast *A. incana*-type includes both *A. incana* and *A. serrulata* with *A.*
615 *serrulata* having a more southern distribution. Thus, it is unclear whether the *Alnus*-peak

616 represents a single event or multiple events closely spaced in time involving different species.
617 Unfortunately, *Alnus* is not consistently separated into the *A. viridis* and *A. incana* types at many
618 sites, making it difficult to resolve this question with existing data. Nevertheless, the *Alnus* types
619 are easily distinguished (Mayle et al., 1993a) and future efforts to separate the pollen types may
620 reveal important paleoecological patterns on a synoptic scale. Plant macrofossils could also help
621 determine particular species involved in important ecological events (Jackson et al. 1997), and
622 could be used in some cases to subdivide pollen taxa into higher-resolution units (e.g., species).
623 We have not yet explored such application. It poses new problems (e.g., subdividing pollen
624 when two or more species are represented by macrofossils; deciding whether the same species
625 are represented locally by macrofossils and regionally by pollen). These problems are
626 surmountable, but would require an additional set of decision rules beyond the scope of our
627 study.

628

629 Across all three ecological events, the slowest rates of ecological change occurred in the region
630 bordering the mid-Atlantic. The *Quercus* rise and *Picea* decline spread at similar rates, with the
631 slowest rates of event propagation in the south, trending northwest, then speeding up in the
632 northeast and upper Midwest. The *Alnus* decline occurred almost simultaneously throughout the
633 northeast, then slowed towards the mid-Atlantic region. Across all three events, the fastest rates
634 of change occurred at the end of the Younger Dryas Chronozone (Figure 6).

635

636 *5.4 Conclusions*

637 Our conceptual framework for ranking ages and our use of benchmark sites as the basis for
638 refined chronologies offers a simple yet rigorous approach to assessing and improving the

639 temporal resolution of mapped vegetation changes. Our error analyses suggest that the effective
640 temporal limit to multisite syntheses of late-Pleistocene vegetation dynamics from fossil pollen
641 records is about 500 years. This resolution is suitable for answering questions at the synoptic
642 scale such as how species and communities responded to abrupt climate change at millennial
643 and, to some degree, sub-millennial time scales. For example, both the Bølling-Allerød and
644 Younger Dryas climatic oscillations lasted over 1000 years, so synoptic patterns of ecological
645 change can be compared before and after rapid climate change at the boundaries of these events.
646 These methods also provide a foundation for a reassessment of how the ecological responses to
647 these climatic changes propagated across large spatial regions. Finally, our identification of
648 benchmark sites helps identify where such sites are sparse and illustrates high-priority regions
649 for future field campaigns. As more benchmark sites and more accurate and precise ages are
650 added, especially in the undersampled regions, the methodological framework established here
651 can be easily used to assess the new limits of mapping and narrow the temporal resolution of
652 future syntheses even further.

653

653 **Acknowledgements**

654 We would like to thank Maarten Blaauw, Simon Brewer, Paul Buckland, Phil Buckland, Thomas
655 Giesecke, Allan Hall, and Alison Smith for discussion of age models, precision, and accuracy.

656 The paper benefitted from comments by Simon Brewer, Thomas Giesecke, Rachel Jones, Mark

657 Lesser, Yao Liu, and two anonymous reviewers. Funding for this project comes from NSF

658 (EAR-0844223, EAR-0843831). A workshop on age models and analysis and visualization tools

659 for the Neotoma Database and related projects was held in Umeå, Sweden in Fall 2010 and

660 funded by The Swedish Research Council, Umeå University Humanities Faculty, and The SEAD

661 Project. Pollen records were obtained from the Neotoma paleoecological database.

662

663

663 **Figures**

664

665 **Figure 1.** Flow chart outlining the search criteria within Neotoma used to identify the initial list
666 of potential benchmark sites in eastern North America (left hand column), and the criteria used to
667 narrow the initial list down to benchmark sites. The specific Neotoma search filters included: 1)
668 Location. Sites within the United States or Canada east of -111° longitude, excluding sites within
669 the states/provinces of Arizona, Northwest Territories, Nunavut, New Mexico. 2) Dataset
670 type=pollen. 3) We excluded sites from the following depositional environments*: Biological
671 (ID #6), Estuarine (ID #16), Playa (ID #47), Coastal (ID #52), Fluvial (ID #77), Stream-cut
672 Exposure (ID #92), Terrestrial (ID #103), Cave (ID #109), Soil (ID #127), Other (ID #136),
673 Unknown (ID #137). 4) Chronology information: We relied on the default chronology,
674 restricting the AgeBoundYounger to $\leq 22,000$ years. All terms and IDs are as in the Neotoma
675 database.

676

677 **Figure 2.** Change point diagram for *Picea* at Crystal Lake, IL (Gonzales and Grimm, 2009). The
678 upper graph shows the original relative abundance, as a proportion of the upland pollen sum (red
679 line) and the posterior mean probability relative abundance (black line). Probable change points
680 (based on BCP analysis) are indicated in filled circles and the change point that we identified as
681 corresponding to each biostratigraphic event is circled. The bottom graph shows the posterior
682 probability of a change point occurring at a given sampling age.

683

684 **Figure 3.** Pollen sites in eastern North America during four different late Pleistocene time
685 periods. All sites in eastern North America that at least partially overlap the time period are

686 shown in black, and the benchmark sites for each time period are shown in red. The number
687 corresponds to the site name: 15, Lake Annie (Watts, 1975); 52, Blackwoods Hollow (Schauffler
688 and Jacobson Jr, 2002); 77, Browns Pond (Kneller and Peteet, 1993); 107, Chase Pond (Mayle et
689 al., 1993b); 117, Chatsworth Bog (Grimm et al., 2009; Nelson et al., 2006); 121, Clear Pond
690 (Hussey, 1993); 130, Conroy Lake (Borns Jr et al., 2004; Doner, 1995); 133, Cottonwood Lake
691 (Barnosky et al., 1987; Grimm et al., 2009); 150, Crystal Lake (Gonzales and Grimm, 2009);
692 162, Decoy Lake (Szeicz and MacDonald, 1991); 172, Devil's Lake (Baker et al., 1992; Grimm
693 et al., 2009; Maher Jr., 2009); 291, Hiscock Site (McAndrews, 2003); 347, Kettle Lake (Brown
694 et al., 2005; Clark et al., 2002; Grimm, 2011); 362, Lac a Magie (Mayle et al., 1993b); 478,
695 Moon Lake (Laird et al., 1996a; Laird et al., 1996b); 492, Mud Pond (Borns Jr et al., 2004;
696 Doner, 1995); 678, Sharkey Lake (Camill et al., 2003); 704, Splan Pond (Mayle et al., 1993b;
697 Mott et al., 1986); 710, Steel Lake, MN (Wright et al., 2004); 720, Sutherland Pond (Maenza-
698 Gmelch, 1997a; Maenza-Gmelch, 1997b); 749, Lake Tulane (Grimm et al., 2006); 789, White
699 Lake (Yu, 2007). ka: thousand years before present.

700

701 **Figure 4.** Interpolated ages of each event for two different methods, inverse distance weighting
702 (IDW-2d) and thin plate splines (TPS-2d). a) *Picea* decline; b) *Alnus* decline; c) *Quercus* rise.

703 Benchmark sites are circled in a thick black line and labeled as in Figure 3.

704

705 **Figure 5.** Comparison of age of each event (based on IDW-2d interpolation) versus the age of
706 the event designated by the default chronology in the Neotoma database. a) *Picea* decline; b)
707 *Alnus* decline; c) *Quercus* rise. Benchmark sites are circled in a thick black line and labeled as in
708 Figure 3.

709

710 **Figure 6.** Contour plots of ecological events, based on linear interpolation of event ages between
711 the benchmark sites. The contours are spaced at 500-year intervals on all three panels.

712

713 **Appendices**

714 **Appendix A.** Table of accuracy codes assigned to all dated material within Neotoma

715 **Appendix B.** List of all sites (n=371) used in the analysis

716

716 **Literature Cited**

- 717 Andree, M., Oeschger, H., Siegenthaler, U., Riesen, T., Moell, M., Ammann, B., Tobolski, K.,
718 1986. 14C dating of plant macrofossils in lake sediment. *Radiocarbon* 28, 411-416.
- 719 APSA Members, 2007. The Australasian Pollen and Spore Atlas V1.0, Australian National
720 University, Canberra. <http://apsa.anu.edu.au/>.
- 721 Baker, R., Maher, L., Chumbley, C., Van Zant, K., 1992. Patterns of Holocene environmental
722 change in the midwestern United States. *Quaternary Res.* 37, 379-389.
- 723 Barnekow, L., Possnert, G., Sandgren, P., 1998. AMS 14C chronologies of Holocene lake
724 sediments in the Abisko area, northern Sweden – a comparison between dated bulk sediment
725 and macrofossil samples. *GFF* 120, 59-67.
- 726 Barnosky, C., Grimm, E., Wright, H., 1987. Towards a postglacial history of the northern Great
727 Plains: A review of the paleoecologic problems. *Annals of the Carnegie Museum* 56, 259-
728 273.
- 729 Barry, D., Hartigan, J., 1993. A Bayesian analysis for change point problems. *Journal of the*
730 *American Statistical Association* 88, 309-319.
- 731 Bennett, K., 1994. Confidence intervals for age estimates and deposition times in late-Quaternary
732 sediment sequences. *The Holocene* 4, 337-348.
- 733 Bennett, K., Fuller, J., 2002. Determining the age of the mid-Holocene *Tsuga canadensis*
734 (hemlock) decline, eastern North America. *The Holocene* 12, 421-429.
- 735 Binney, H., Edwards, M.E., Willis, K.J., 2008. Establishing a Northern Eurasian paleoecological
736 database: The pollen data. *PAGES News* 16, 34.

737 Birks, H., Ammann, B., 2000. Two terrestrial records of rapid climatic change during the glacial-
738 Holocene transition (14,000-9,000 calendar years B.P.) from Europe. *Proc. Natl Acad. Sci.*
739 *USA* 97, 1390-1394.

740 Blaauw, M., 2010a. Methods and code for 'classical' age-modelling of radiocarbon sequences.
741 *Quaternary Geochronology* 5, 512-518.

742 Blaauw, M., 2010b. Out of tune: the dangers of aligning proxy archives. *Quaternary Science*
743 *Reviews* doi: 10.1016/j.quascirev.2010.11.012.

744 Borns Jr, H.W., Doner, L.A., Dorion, C.C., Jacobson Jr, G.L., Kaplan, M.R., Kreutz, K.J.,
745 Lowell, T.V., Thompson, W.B., Weddle, T.K., Ehlers, J., Gibbard, P.L., 2004. The
746 deglaciation of Maine, U.S.A, *Developments in Quaternary Science*. Elsevier, pp. 89-109.

747 Bronk Ramsey, C., 2008. Radiocarbon dating: Revolutions in understanding. *Archaeometry* 50,
748 249-275.

749 Brown, K.J., Clark, J., Grimm, E., Donovan, J., Mueller, P., Hansen, B., Stefanova, I., 2005. Fire
750 cycles in North American interior grasslands and their relation to prairie drought. *Proc. Natl*
751 *Acad. Sci. USA* 102, 8865-8870.

752 Camill, P., Umbanhowar Jr, C., Teed, R., Geiss, C., Aldinger, J., Dvorak, L., Kenning, J.,
753 Limmer, J., Walkup, K., 2003. Late-glacial and Holocene climatic effects on fire and
754 vegetation dynamics at the prairie-forest ecotone in south-central Minnesota. *Journal of*
755 *Ecology* 91, 822-836.

756 Clark, J., Grimm, E.C., Donovan, J.J., Fritz, S., Engstrom, D., Almendinger, J., 2002. Drought
757 cycles and landscape responses to past aridity on prairies of the northern Great Plains, USA.
758 *Ecology* 83, 595-601.

759 Cushing, E.J., 1967. Late-Wisconsin pollen stratigraphy in the glacial sequence in Minnesota, In:
760 Cushing, E.J., Wright, H.E., Jr (Eds.), Quaternary paleoecology. Yale University Press, New
761 Haven, pp. 59-88.

762 Damon, P.E., Lerman, J.C., Long, A., 1978. Temporal fluctuations of atmospheric ^{14}C : causal
763 factors and implications. *Annu. Rev. Earth Pl. Sc.* 6, 457-494.

764 Davis, M.B., 1976. Pleistocene biogeography of temperate deciduous forests. *Geoscience and*
765 *Man* XIII, 13-26.

766 Deevey, E.S., Jr., 1939. Studies on Connecticut lake sediments. I. A postglacial climatic
767 chronology for southern New England. *American Journal of Science* 237, 691-724.

768 Deevey Jr, E.S., Gross, M.S., Hutchinson, G.E., Kraybill, H.L., 1954. The natural C^{14} contents
769 of materials from hard-water lakes. *Proc. Natl Acad. Sci. USA* 40, 285-288.

770 Denton, G.H., Anderson, R.S., Toggweiler, J.R., Edwards, R.L., Schaefer, J.M., Putnam, A.E.,
771 2010. The last glacial termination. *Science* 328, 1652-1656.

772 Dietl, G.P., Flessa, K.W., 2011. Conservation paleobiology: putting the dead to work. *Trends*
773 *Ecol. Evol.*

774 Doner, L.A., 1995. Late-Pleistocene environments in Maine and the Younger Dryas dilemma.
775 University of Maine, Orono, Maine, USA.

776 Emerson, J.W., Erdman, C., 2007. bcp: An R Package for Performing a Bayesian Analysis of
777 Change Point Problems. *Journal of Statistical Software* 23, 1-13.

778 Firbas, F., 1950. The Late-Glacial Vegetation of Central Europe. *New Phytologist* 49, 163-173.

779 Flessa, K.W., Jackson, S.T., 2005. The geological record of ecological dynamics: understanding
780 the biotic effects of future environmental change. National Academy Press, Washington,
781 D.C.

782 Fyfe, R., de Beaulieu, J.L., Binney, H., Bradshaw, R., Brewer, S., Le Flao, A., Finsinger, W.,
783 Gaillard, M., Giesecke, T., Gil-Romera, G., 2009. The European Pollen Database: past
784 efforts and current activities. *Vegetation History and Archaeobotany* 18, 417-424.

785 Gavin, D., 2001. Estimation of inbuilt age in radiocarbon ages of soil charcoal for fire history
786 studies. *Radiocarbon* 43, 27-44.

787 Gonzales, L.M., Grimm, E., 2009. Synchronization of late-glacial vegetation changes at Crystal
788 Lake, Illinois, USA with the North Atlantic Event Stratigraphy. *Quaternary Res.* 72, 234-245.

789 Grimm, E., 2011. High-resolution age model based on AMS radiocarbon ages for Kettle Lake,
790 North Dakota, USA. *Radiocarbon* 53.

791 Grimm, E., Jacobson, G., 2003. Late-Quaternary vegetation history of the eastern United States,
792 In: Gillespie, A.R., Porter, S.C., Atwater, B.F. (Eds.), *The Quaternary Period in the United*
793 *States*. Elsevier, Amsterdam, pp. 381-402.

794 Grimm, E., Maher Jr, L., Nelson, D., 2009. The magnitude of error in conventional bulk-
795 sediment radiocarbon dates from central North America. *Quaternary Res.* 72, 301-308.

796 Grimm, E., Watts, W., Jacobson Jr, G., Hansen, B., Almquist, H., Dieffenbacher-Krall, A., 2006.
797 Evidence for warm wet Heinrich events in Florida. *Quaternary Science Reviews* 25, 2197-
798 2211.

799 Grimm, E.C., Jacobson, G.L., Jr., 1992. Fossil-pollen evidence for abrupt climate changes during
800 the past 18 000 years in eastern North America. *Climate Dynamics* 6, 179-184.

801 Grimm, E.C., Keltner, J., Cheddadi, R., Hicks, S., Lézine, A.-M., Berrio, J.C., Williams, J.W.,
802 2007. Pollen databases and their application, In: Elias, S.A. (Ed.), *Encyclopedia of*
803 *Quaternary science*. Elsevier, Amsterdam,, pp. 2522-2530

804 Haslett, J., Parnell, A., 2008. A simple monotone process with application to radiocarbon-dated
805 depth chronologies. *Journal of the Royal Statistical Society: Series C (Applied Statistics)* 57,
806 399-418.

807 Hopkins, A.D., 1920. The bioclimatic law. *Monthly Weather Review* 48, 355.

808 Huntley, B., Birks, H.J.B., 1983. *An Atlas of Past and Present Pollen Maps for Europe: 0-13000*
809 *Years Ago*. Cambridge University Press, Cambridge.

810 Hussey, T.C., 1993. A 20,000 year history of vegetation and climate at Clear Pond, northeastern
811 South Carolina. University of Maine, Orono, Maine, USA.

812 Jackson, S., Whitehead, D., 1993. Pollen and macrofossils from Wisconsinan interstadial
813 sediments in northeastern Georgia. *Quaternary Res.* 39, 99-106.

814 Jackson, S.T., Webb, R.S., Anderson, K.H., Overpeck, J.T., Webb III, T., Williams, J.W.,
815 Hansen, B., 2000. Vegetation and environment in Eastern North America during the Last
816 Glacial Maximum. *Quaternary Science Reviews* 19, 489-508.

817 Jacobson, G.L., Jr., Webb, T., III, Grimm, E.C., 1987. Patterns and rates of vegetation change
818 during the deglaciation of eastern North America, In: W.F. Ruddiman, Wright, H.E., Jr.
819 (Eds.), *North America and Adjacent Oceans During the Last Deglaciation*. Geological
820 Society of America, Boulder, pp. 277-288.

821 Kneller, M., Peteet, D., 1993. Late-Quaternary climate in the Ridge and Valley of Virginia,
822 U.S.A.: Changes in vegetation and depositional environment. *Quaternary Science Reviews*
823 12, 613-628.

824 Laird, K., Fritz, S., Grimm, E., Mueller, P., 1996a. Century-scale paleoclimatic reconstruction
825 from Moon Lake, a closed-basin lake in the northern Great Plains. *Limnology and*
826 *Oceanography* 41, 890-902.

- 827 Laird, K.R., Fritz, S.C., Maasch, K., Cumming, B.F., 1996b. Greater drought intensity and
828 frequency before AD 1200 in the Northern Great Plains, USA. *Nature* 384, 552-554.
- 829 Lowe, J.J., Lowe, S., Fowler, A.J., Hedges, R.E.M., Austin, T.J.F., 1988. Comparison of
830 accelerator and radiometric ^{14}C measurements obtained from Late Devensian lateglacial
831 lake sediments from Llyn Gwernan, North Wales, UK. *Boreas* 17, 355-369.
- 832 MacArthur, R.H., 1972. *Geographical ecology; patterns in the distribution of species*. Harper and
833 Row, New York.
- 834 MacDonald, G.M., Beukens, R.P., Kieser, W.E., 1991. Radiocarbon dating of limnic sediments:
835 A comparative analysis and discussion. *Ecology* 72, 1150-1155.
- 836 Maenza-Gmelch, T., 1997a. Late-glacial-early Holocene vegetation, climate, and fire at
837 Sutherland Pond, Hudson Highlands, southeastern New York, USA. *Canadian Journal of*
838 *Botany* 75, 431-439.
- 839 Maenza-Gmelch, T.E., 1997b. Holocene vegetation, climate, and fire history of the Hudson
840 Highlands, southeastern New York, USA. *The Holocene* 7, 25-37.
- 841 Maher Jr., L.J., 2009. The palynology of Devils Lake, Sauk County, Wisconsin, In: Knox, J.C.,
842 Clayton, L., Mickelson, D.M. (Eds.), *Quaternary history of the Driftless Area: Wisconsin*
843 *geological and natural history survey field trip guide B*, pp. 119-135.
- 844 Mayle, F., Levesque, A., Cwynar, L., 1993a. *Alnus* as an indicator taxon of the Younger Dryas
845 cooling in eastern North America. *Quaternary Science Reviews* 12, 295-305.
- 846 Mayle, F.E., Levesque, A., Cwynar, L.C., 1993b. Accelerator-mass-spectrometer ages for the
847 Younger Dryas event in Atlantic Canada. *Quaternary Res.* 39, 355-360.
- 848 McAndrews, J.H., 2003. Postglacial ecology of the Hiscock Site, In: Laub, R.S. (Ed.), *The*
849 *Hiscock Site: Late Pleistocene and Holocene Paleoecology and Archaeology of Western*

850 New York State. Bulletin of the Buffalo Society of Natural Sciences, Buffalo, NY, pp. 190–
851 198.

852 Meltzer, D.J., Mead, J.I., 1983. The timing of late Pleistocene mammalian extinctions in North
853 America. *Quaternary Res.* 19, 130-135.

854 Mott, R., Grant, D., Stea, R., Occhietti, S., 1986. Late-glacial climatic oscillation in Atlantic
855 Canada equivalent to the Allerød/Younger Dryas event. *Nature* 323, 247-250.

856 Nelson, D., Hu, F., Grimm, E., Curry, B., Slate, J., 2006. The influence of aridity and fire on
857 Holocene prairie communities in the eastern Prairie Peninsula. *Ecology* 87, 2523-2536.

858 Oswald, W., Faison, E., Foster, D., Doughty, E., Hall, B., Hansen, B., 2007. Post-glacial changes
859 in spatial patterns of vegetation across southern New England. *J. Biogeogr.* 34, 900-913.

860 Oswald, W.W., Anderson, P.M., Brown, T.A., Brubaker, L.B., Hu, F.S., Lozhkin, A.V., Tinner,
861 W., Kaltenrieder, P., 2005. Effects of sample mass and macrofossil type on ¹⁴C dating of
862 arctic and boreal lake sediments. *The Holocene* 15, 758-767.

863 Overpeck, J.T., Whitlock, C., Huntley, B., 2003. Terrestrial biosphere dynamics in the climate
864 system; past and future, In: Bradley, R.S., Pedersen, T.F., Alverson, K.D., Bergmann, K.F.
865 (Eds.), *Paleoclimate, global change and the future*. Springer-Verlag, Berlin, pp. 81-103.

866 Parnell, A., Haslett, J., Allen, J., Buck, C., Huntley, B., 2008. A flexible approach to assessing
867 synchronicity of past events using Bayesian reconstructions of sedimentation history.
868 *Quaternary Science Reviews* 27, 1872-1885.

869 Peros, M.C., Gajewski, K., Viau, A.E., 2008. Continental-scale tree population response to rapid
870 climate change, competition and disturbance. *Global Ecology and Biogeography* 17, 658-
871 669.

872 Pettitt, P., Davies, W., Gamble, C., Richards, M., 2003. Palaeolithic radiocarbon chronology:
873 quantifying our confidence beyond two half-lives. *Journal of Archaeological Science* 30,
874 1685-1693.

875 R Development Core Team, 2010. R: A language and environment for statistical computing. R
876 Foundation for Statistical Computing, Vienna, Austria.

877 Reimer, P., Baillie, M., Bard, E., Bayliss, A., Beck, J., Blackwell, P., Ramsey, C., Buck, C.,
878 Burr, G., Edwards, R., Friedrich, M., Grootes, P.M., Guilderson, T.P., Hajdas, I., Heaton,
879 T.J., Hogg, A.G., Hughen, K.A., Kaiser, K.F., Kromer, B., McCormac, F.G., Manning, S.W.,
880 Reimer, R.W., Richards, D.A., Southon, J.R., Talamo, S., Turney, C.S.M., van der Plicht, J.,
881 Weyhenmeyer, C.E., 2009. IntCal09 and Marine09 radiocarbon age calibration curves, 0-
882 50,000 years cal BP. *Radiocarbon* 51, 1111-1150.

883 Santos, G.M., Southon, J.R., Griffin, S., Beaupre, S.R., Druffel, E.R.M., 2007. Ultra small-mass
884 AMS 14C sample preparation and analyses at KCCAMS/UCI Facility. *Nuclear Instruments*
885 *and Methods in Physics Research B* 259, 293-302.

886 Schauffler, M., Jacobson Jr, G., 2002. Persistence of coastal spruce refugia during the Holocene
887 in northern New England, USA, detected by stand-scale pollen stratigraphies. *Journal of*
888 *Ecology* 90, 235-250.

889 Shuman, B., Bartlein, P., Webb III, T., 2005. The magnitudes of millennial-and orbital-scale
890 climatic change in eastern North America during the Late Quaternary. *Quaternary Science*
891 *Reviews* 24, 2194-2206.

892 Shuman, B., Webb Iii, T., Bartlein, P., Williams, J.W., 2002. The anatomy of a climatic
893 oscillation: vegetation change in eastern North America during the Younger Dryas
894 chronozone. *Quaternary Science Reviews* 21, 1777-1791.

895 Smith, A., Pilcher, J., 1973. Radiocarbon dates and vegetational history of the British Isles. *New*
896 *Phytologist* 72, 903-914.

897 Solomon, S., Qin, D., Manning, M., Chen, Z., Marquis, M., Averyt, K.B., Tignor, M., Miller,
898 H.L., 2007. *Climate Change 2007: The Physical Science Basis. Contribution of Working*
899 *Group I to the Fourth Assessment Report of the Intergovernmental Panel on Climate Change*
900 *Cambridge University Press, New York.*

901 Stafford Jr, T., Jull, A., Brendel, K., Duhamel, R., Donahue, D., 1987. Study of bone radiocarbon
902 dating accuracy at the University of Arizona NSF Accelerator Facility for Radioisotope
903 Analysis. *Radiocarbon* 29, 24-44.

904 Stuiver, M., Reimer, P.J., 1993. Extended ^{14}C database and revised CALIB radiocarbon
905 calibration program. *Radiocarbon* 35, 215-230.

906 Szeicz, J., MacDonald, G., 1991. Postglacial vegetation history of oak savanna in southern
907 Ontario. *Canadian Journal of Botany* 69, 1507-1519.

908 Tian, J., Brown, T., Hul, F., 2005. Comparison of varve and ^{14}C chronologies from Steel Lake,
909 Minnesota, USA. *The Holocene* 15, 510.

910 Turney, C., Coope, G., Harkness, D., Lowe, J., Walker, M., 2000. Implications for the dating of
911 Wisconsinan (Weichselian) Late-Glacial events of systematic radiocarbon age differences
912 between terrestrial plant macrofossils from a site in SW Ireland. *Quaternary Res.* 53, 114-
913 121.

914 von Post, L., 1946. The prospect for pollen analysis in the study of Earth's climatic history. *New*
915 *Phytologist* 45, 193-217.

916 Watts, W.A., 1975. A late Quaternary record of vegetation from Lake Annie, south-central
917 Florida. *Geology* 3, 344-346.

918 Watts, W.A., 1980. The late Quaternary vegetation history of the southeastern United States.
919 Annual Review of Ecology and Systematics 11, 387-409.

920 Williams, J., Post, D.M., Cwynar, L.C., Lotter, A.F., Levesque, A.J., 2002. Rapid and
921 widespread vegetation responses to past climate change in the North Atlantic region.
922 Geology 30, 971-974.

923 Williams, J.W., Blois, J.L., Shuman, B.N., in press. Extrinsic and intrinsic forcing of abrupt
924 ecological change: Case studies from the late Quaternary. Journal of Ecology.

925 Williams, J.W., Shuman, B., Webb III, T., Bartlein, P.J., Leduc, P.L., 2004. Late-Quaternary
926 vegetation dynamics in North America: Scaling from taxa to biomes. Ecological Monographs
927 74, 309-334.

928 Willis, K., Bailey, R., Bhagwat, S., Birks, H., 2010. Biodiversity baselines, thresholds and
929 resilience: testing predictions and assumptions using palaeoecological data. Trends Ecol.
930 Evol. 25, 583-591.

931 Wright, H., Stefanova, I., Tian, J., Brown, T.A., Hu, F.S., 2004. A chronological framework for
932 the Holocene vegetational history of central Minnesota: the Steel Lake pollen record.
933 Quaternary Science Reviews 23, 611-626.

934 Yu, Z., 2007. Rapid response of forested vegetation to multiple climatic oscillations during the
935 last deglaciation in the northeastern United States. Quaternary Res. 67, 297-303.

936

937

938

938 **Tables**

939

940 **Table 1.** Accuracy and precision ranks assigned to each ¹⁴C age. Benchmark sites had at least
 941 one ¹⁴C age within 1000 years of the time period of interest with accuracy less than or equal to
 942 rank 4 and precision less than or equal to rank 5.

Rank	Accuracy	Precision
	The true age of event and estimated age may be systematically offset by:	The calibrated age range is:
1	≤1 years	≤1 years
2	≤10 years	≤10 years
3	≤100 years	≤100 years
4	≤250 years	≤250 years
5	≤500 years	≤500 years
6	≤1000 years	≤1000 years
7	≤5000 years	≤5000 years
8	>5000 years	>5000 years

943

944

944 **Table 2.** The correlation between the site-specific cross-validation age error with the original age
 945 of the event, original age range, latitude, longitude, and altitude, for *Picea* decline, *Alnus* decline,
 946 and *Quercus* rise. The r-value is listed first, followed by the P-value. Significant correlations
 947 are shown in bold.

948

	<u><i>Picea</i> Decline</u>		<u><i>Alnus</i> Decline</u>		<u><i>Quercus</i> Rise</u>	
	IDW-2d	TPS-2d	IDW-2d	TPS-2d	IDW-2d	TPS-2d
Original age	-0.976; 0	-0.847; 0	-0.847; 0.001	-0.503; 0.096	-0.948; 0	-0.832; 0.000
Age range	-0.411; 0.128	-0.277; 0.317	0.437; 0.155	0.425; 0.169	-0.567; 0.035	-0.362; 0.203
Latitude	0.596; 0.019	0.391; 0.150	-0.002; 0.996	0.462; 0.131	0.601; 0.023	0.401; 0.156
Longitude	-0.147; 0.602	-0.230; 0.312	-0.083; 0.798	-0.118; 0.716	-0.096; 0.745	-0.031; 0.916
Altitude	0.434; 0.106	0.633; 0.011	0.681; 0.015	0.589; 0.044	0.412; 0.143	0.404; 0.152

949

950

951

951 **Table 3.** Cross-validation and correlation statistics for three biostratigraphic events, for
 952 benchmark sites only. For the *Alnus* decline, the southern sites are defined as Clear Pond, SC
 953 and Browns Pond, VA. ME: Mean error; RMSE: Root mean square error; MAE: Mean Absolute
 954 Error; Extrapolation MAE: MAE at sites at the boundary of the interpolation range; Interpolation
 955 MAE: MAE at sites within the boundary of the interpolation range. Interpolation MAE is the
 956 most appropriate metric of interpolation error (see text).

a. <i>Picea</i> Decline	<u>All sites</u>		<u>CLEARPOND removed</u>	
	IDW-2d	TPS-2d	IDW-2d	TPS-2d
MAE	842	1038	450	453
Extrapolation MAE	1582	1843	307	439
Interpolation MAE	574	746	530	461
b. <i>Alnus</i> decline	<u>All sites</u>		<u>Southern sites removed</u>	
	IDW-2d	TPS-2d	IDW-2d	TPS-2d
MAE	367	720	325	563
Extrapolation MAE	398	1416	323	794
Interpolation MAE	352	372	327	410
c. <i>Quercus</i> Rise	<u>All sites</u>		<u>CLEARPOND removed</u>	
	IDW-2d	TPS-2d	IDW-2d	TPS-2d
MAE	1012	947	637	743
Extrapolation MAE	2110	1697	664	784
Interpolation MAE	573	647	614	709

957

957 **Table 4.** Comparison of biostratigraphic versus original ages, for all sites. All statistics are
 958 calculated on the difference between the original age of an event estimated by change point
 959 analysis and the event age estimated by interpolation (IDW-2d).

	Mean	Standard Deviation	Minimum	Maximum	Mean Absolute Difference
<i>Picea decline</i>	-287	1134	-4353	2889	845
<i>Alnus decline</i>	33	1532	-4059	4566	858
<i>Quercus rise</i>	-287	1650	-3676	4842	1106

960

Figure 1

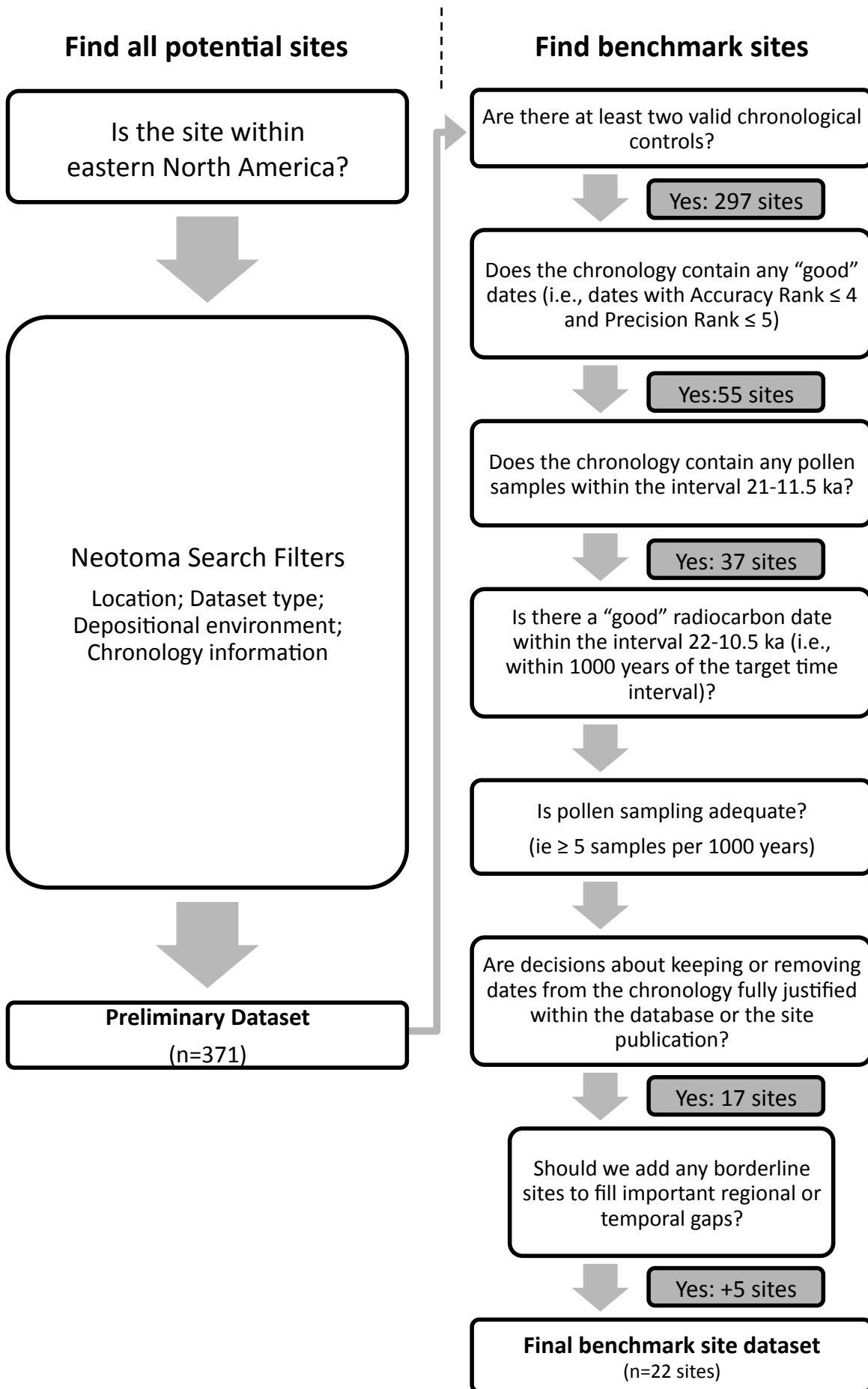


Figure 2

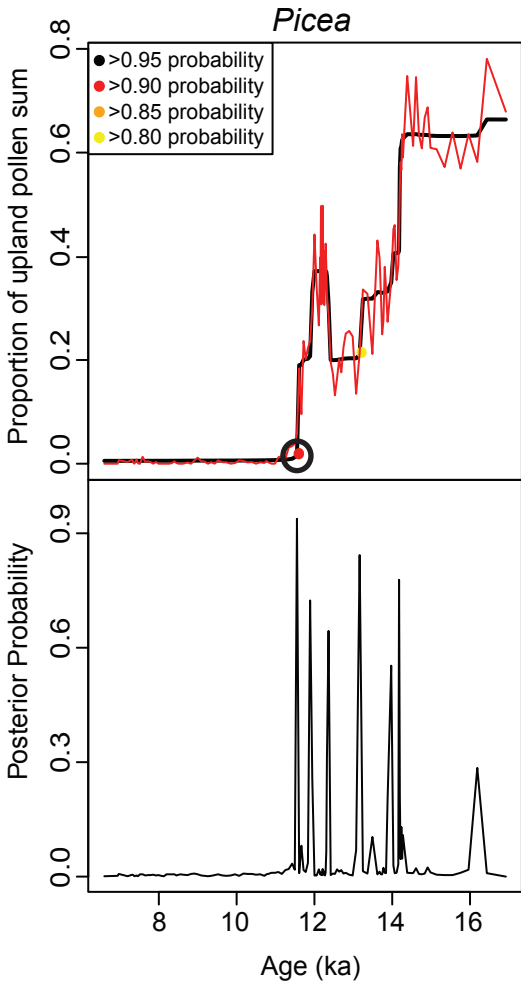


Figure 3

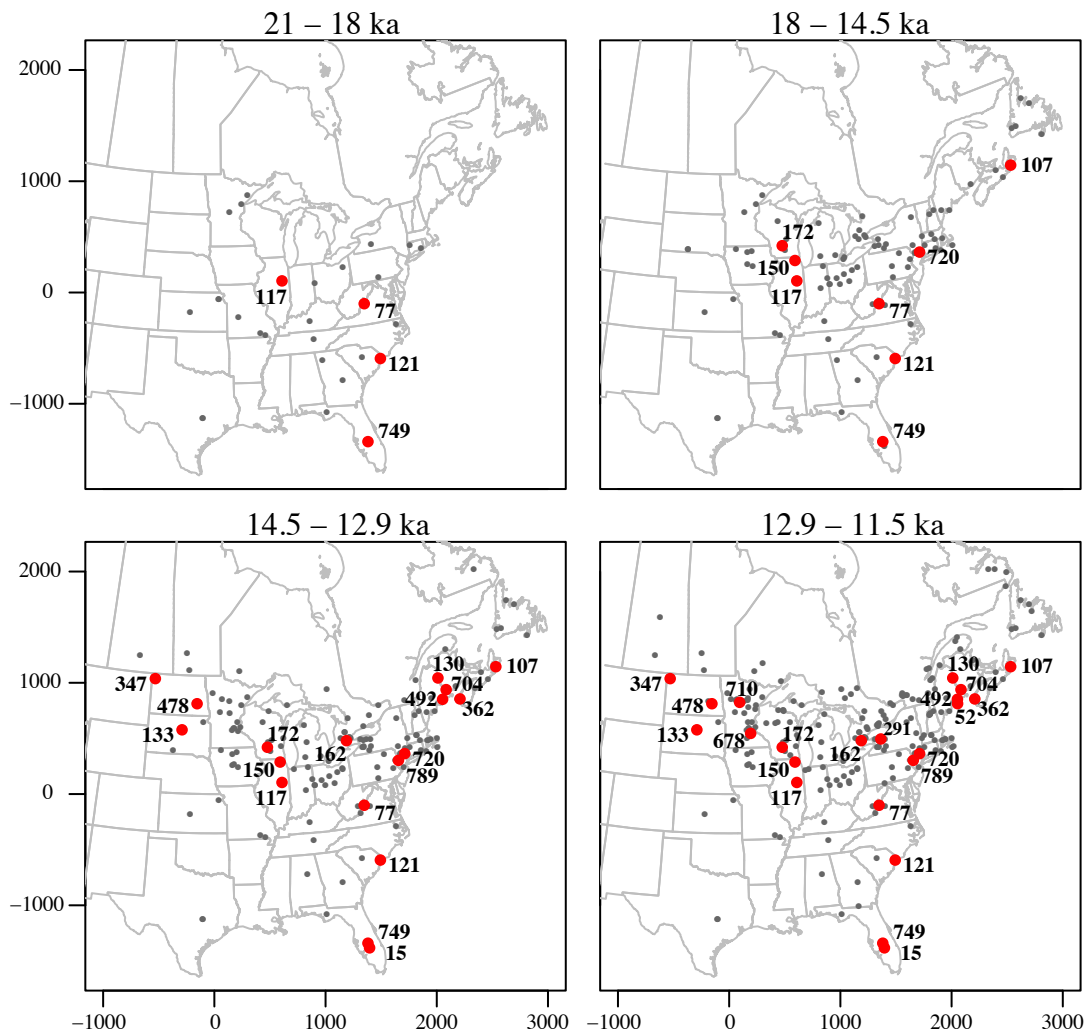


Figure 4

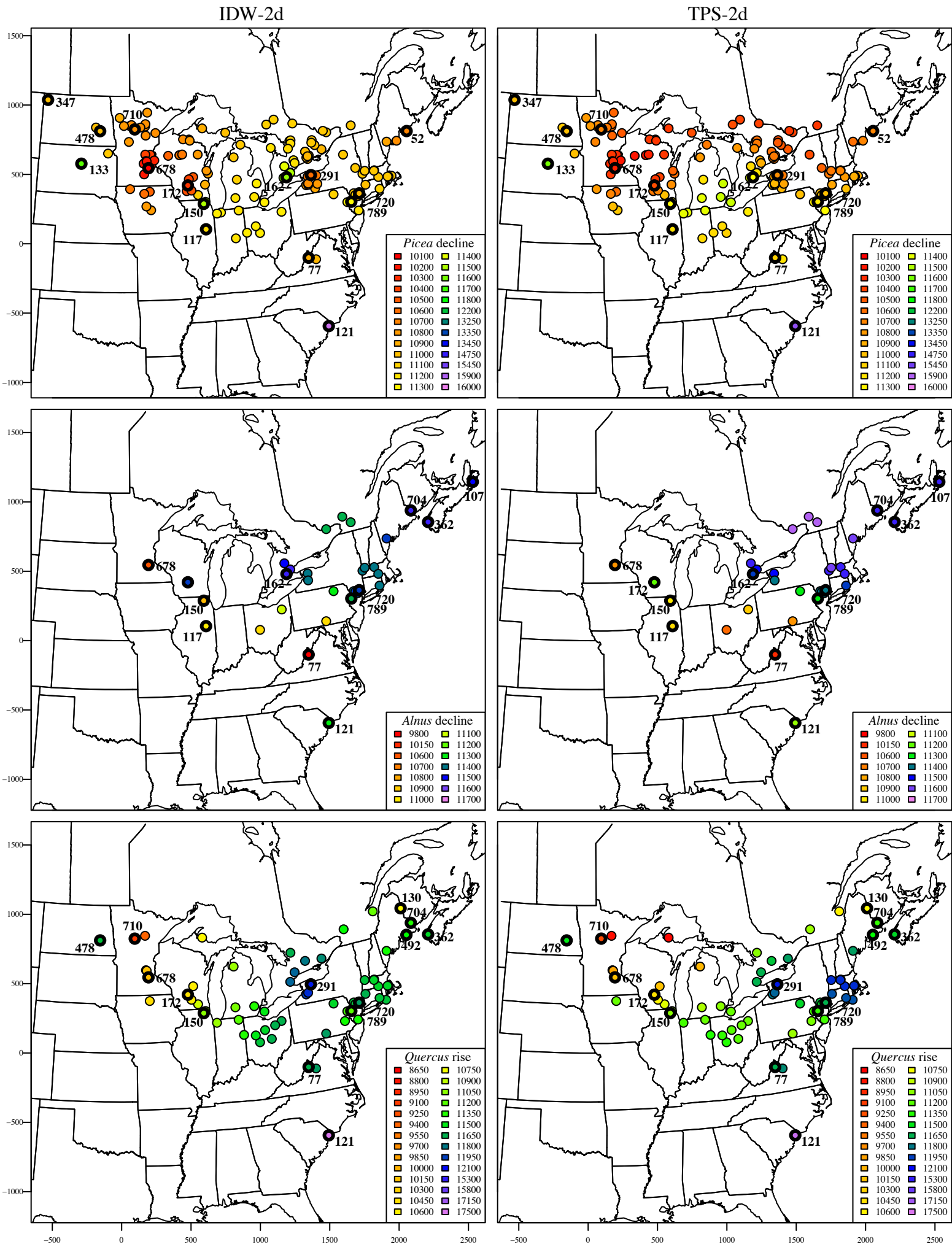


Figure 5

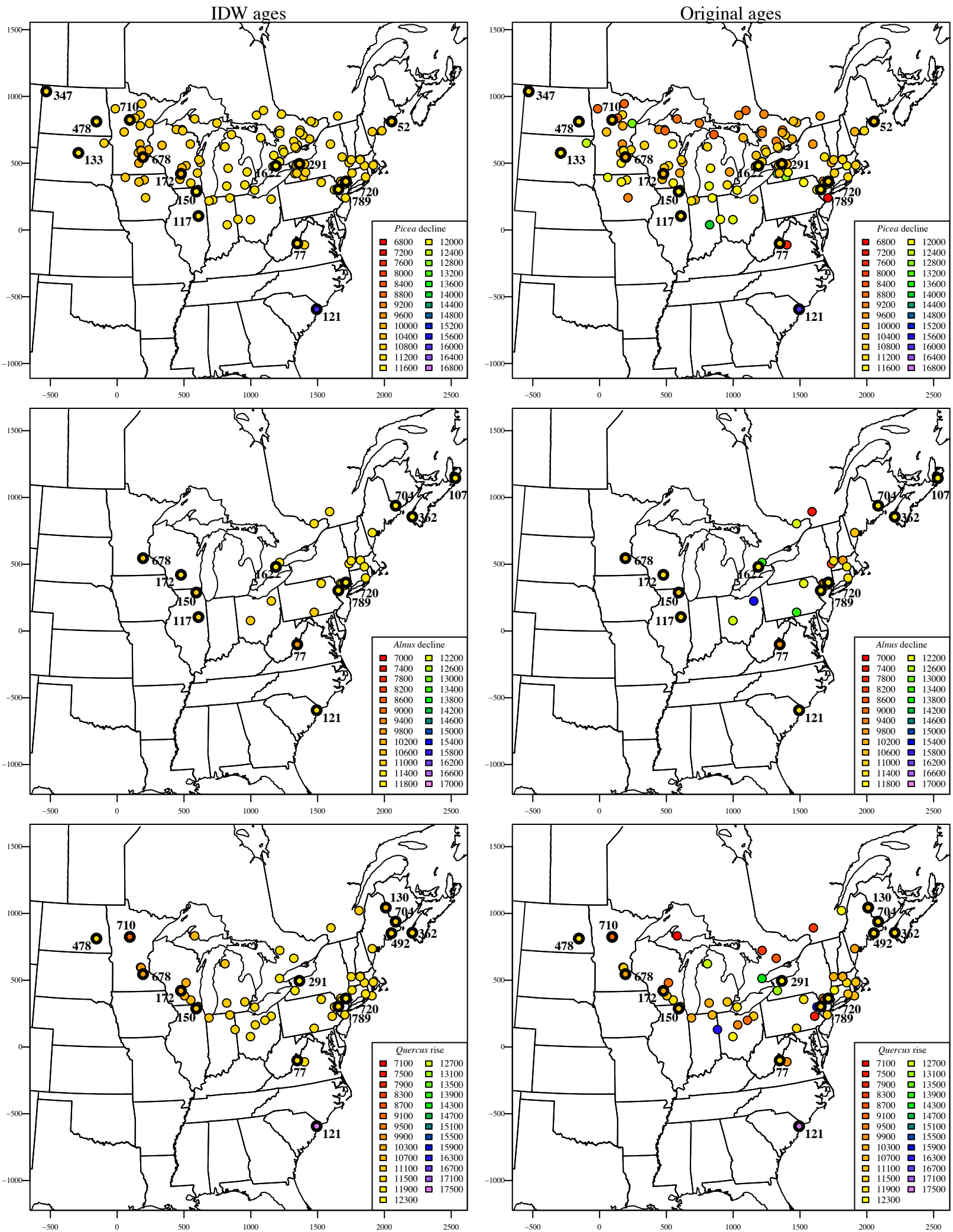


Fig. 6

